



Published in final edited form as:

*J Sustain Min.* 2019 May ; 18: 100–108. doi:10.1016/j.jsm.2019.02.008.

## A field study on the possible attachment of DPM and respirable dust in mining environments

Sallie Gaillard<sup>a</sup>, Emily Sarver<sup>a,\*</sup>, Emanuele Cauda<sup>b</sup>

<sup>a</sup>Virginia Tech, Department of Mining and Minerals Engineering, Blacksburg, VA, 24060, USA

<sup>b</sup>CDC/NIOSH Office of Mine Safety and Health Research (OMSHR), Pittsburgh, PA, 15236, USA

### Abstract

Typical monitoring procedures for diesel particulate matter (DPM) in mines include the collection of filter samples using particle size selectors. The size selectors are meant to separate the DPM, which is generally considered to occur in the submicron range (i.e.,  $< 0.8 \mu\text{m}$ ), from larger dust particles that could present analytical interferences. However, previous studies have demonstrated that this approach can sometimes result in undersampling, therefore, excluding significant fractions of the DPM mass. The excluded fraction may represent oversized DPM particles, but another possibility is that submicron DPM attaches to supramicron dust particles such that it is *effectively* oversized. To gain insights into this possibility, a field study was conducted in an underground stone mine. Submicron, respirable, and total airborne particulate filter samples were collected in three locations to determine elemental carbon (EC) and total carbon (TC), which are commonly used as analytical surrogates for DPM. Concurrent with the collection of the filter samples, a low-flow sampler with an electrostatic precipitator was also used to collect airborne particulates onto 400-mesh copper grids for analysis by transmission electron microscope (TEM). Results indicated that, while typical submicron sampling did account for the majority of DPM mass in the study mine, DPM-dust attachment can indeed occur. The effect of exposure to such attached particulates has not been widely investigated.

### Keywords

Diesel particulate matter; Dust; Transmission electron microscope; NIOSH method 5040; Submicron particles

---

This is an open access article under the CC BY-NC-ND license (<http://creativecommons.org/licenses/by-nc-nd/4.0/>).

\*Corresponding author. Virginia Tech, Department of Mining and Minerals Engineering, 108A Holden Hall, 445 Old Turner Street, Blacksburg, VA, 24061, USA. [esarver@vt.edu](mailto:esarver@vt.edu) (E. Sarver).

Conflicts of interest

None.

Ethical statement

Authors state that the research was conducted according to ethical standards.

Disclaimer

The findings and conclusions in this paper are those of the authors and do not necessarily represent the official position of the National Institute for Occupational Safety and Health (NIOSH), Centers for Disease Control and Prevention. Mention of company names or products does not constitute endorsement by NIOSH.

## 1. Introduction

### 1.1. DPM sampling in mines

Diesel particulate matter (DPM) is a significant occupational health hazard for underground mine workers (Cantrell & Rubow, 1991; Cantrell & Watts, 1997). DPM is largely comprised of elemental carbon (EC) and organic carbon (OC), which have been observed to occur in a relatively constant ratio in mine settings (Abdul-Khalek, Kittelson, Graskow, Wei, & Bear, 1998, p. 980525; Kittelson, 1998; Noll, Bugarski, Patts, Mischler, & McWilliams, 2007). For this reason, EC and total carbon (TC, taken as the sum of EC and OC) have been established as suitable surrogates for monitoring DPM (MSHA, 2008). In metal and non-metal mines in the U.S., the Mine Safety and Health Administration (MSHA) regulates a personal exposure limit of 160  $\mu\text{g}/\text{m}^3$  of TC on an 8-h time-weighted average basis (MSHA, 2008). To measure TC, filter samples are collected and analyzed by the NIOSH 5040 standard method (Birch, 2016; MSHA, 2008). This is a thermal-optical method that includes a series of temperature ramps in first a helium atmosphere and then an oxygen atmosphere to drive off the OC and then EC, respectively; any EC created from the thermal decomposition of OC is corrected by tracking laser transmittance changes on the sample filter during analysis (Birch, 2016).

Mine atmospheres generally have significant airborne dust concentrations, which can interfere with 5040 analysis (Noll, Janisko, & Mischler, 2013; Noll, Timko, McWilliams, Hall, & Haney, 2005; Vermeulen et al., 2010). Mineral dusts with carbonate content can be thermally decomposed in the OC measurement step of the 5040 method, effectively increasing the TC result. Mineral dusts with refractory minerals may also affect the optical measurements during the analysis (Birch, 2016). To address the problem of carbonate interference, the carbonate carbon can be removed from the sample by acidification prior to 5040 analysis, or it can be removed analytically from the 5040 result (Birch, 2016); however, these approaches have not been favored in practice. Another approach, and one which applies to all dust types, is the use of a particle size selector during sampling. Devices such as the DPM impactor (DPMI; SKC, Eighty Four, PA) are designed to remove larger particles from the sample stream, so that only particles smaller than the device's cut size (i.e., 0.8  $\mu\text{m}$  at a flow rate of 1.7 LPM) are deposited on the sample filter. This approach, thus, takes advantage of the size difference that generally exists between DPM, which is mostly in the submicron range, and dust, which is mostly in the supramicron range (Cantrell & Rubow, 1991; Cantrell & Watts, 1997; Noll et al., 2005).

There is of course no perfect cut size to completely segregate one particle type from the other. It is well established that DPM occurs in two primary modes: the nuclei mode includes nano-sized (i.e., less than 50 nm) particles of semi-volatile organic compounds, and the accumulation mode includes spherical soot particles that agglomerate together in globs and chains, often with adsorbed organics (Abdul-Khalek et al., 1998, p. 980525; Bukowiecki et al., 2002; Cantrell & Watts, 1997; Kittelson, 1998; Pietikainen et al., 2009). The nuclei mode represents about 90% of DPM by particle number, while the accumulation mode accounts for most of the DPM mass (Abdul-Khalek et al., 1998, p. 980525; Kittelson, 1998). Only a small fraction of DPM particles (i.e., 5–20% by mass) are larger than about 1  $\mu\text{m}$ ,

and these are formed by continued agglomeration under conditions that allow for relatively long residence times with high particle concentrations (Cantrell & Watts, 1997; Bukowiecki et al., 2002; Chou, Chen, Huang, & Liu, 2003). On the other hand, dust generated in many mine environments tends to be mostly greater than about 1  $\mu\text{m}$  (Cantrell & Watts, 1997).

## 1.2. Potential for under-sampling of DPM

Considering these general size ranges, the size selector approach to DPM sampling has proven to be quite efficient in limiting mineral dust interferences in 5040 analysis (Noll et al., 2005; 2013). However, there is a potential to miss some of the DPM. Anecdotally, this is evident in the gradual blackening appearance of a DPMSI with use, or the collection of black particulates in the grit pot of a cyclone size selector. Inadvertent DPM removal when using a size selector can happen if the device, by virtue of its design, actually removes some DPM; if the DPM itself is larger than the selector's cut size; or if the DPM is effectively larger than the cut size because it is attached to larger particles. Removal of DPM in the size selector may be an issue, for example, in cases where an impactor is used excessively. As the impactor begins to load with particulates, including DPM, the effect becomes increasingly worse because the impactor's cut size is gradually reduced (Cauda, Sheehan, Gussman, Kenny, & Volkwein, 2014; Gaillard, Sarver, & Cauda, 2018). Moreover, in cases where tubing must be used between the size selector and filter cassette (e.g., in real-time monitoring instruments like the FLIR Airtec), the tubing can also remove some DPM. Conductive tubing is often recommended to minimize this problem (Noll et al., 2013).

The case of oversized DPM has also been considered (Cantrell & Rubow, 1991; Vermeulen et al., 2010). Vermeulen et al. (2010) conducted extensive work in seven non-metal mines to collect submicron (i.e., using an impactor), respirable (i.e., using a Dorr-Oliver cyclone), to remove all particles greater than 10  $\mu\text{m}$  and yield a  $d_{50}$  cut size of about 3.5  $\mu\text{m}$ , and total particulates (i.e., using an open-face cassette). Their results showed that respirable and total EC were generally similar, but submicron EC was consistently less than respirable EC. Specifically, submicron EC was 77% of respirable EC, on average, though this figure varied between 54% and 84%. These results indicate that some DPM is missed by typical sampling procedures, and are consistent with others where a similar experimental approach (i.e., measurements using different sampling trains) was used in the laboratory or in the field (e.g., Noll et al., 2005).

Although exclusion of oversized DPM during sampling has commonly been attributed to the size of the DPM itself, the attachment of DPM and dust could also be a contributing factor. In a laboratory study aimed at measuring airborne DPM in the presence of mineral dust particles, Noll et al. (2013) suggested that coagulation (i.e., attachment) between DPM and dust might cause less DPM to be collected on sample filters when using an impactor than when not using it. To specifically investigate this possibility of mixed aerosol exposures, Cauda, Miller, Stabile, and Buonanno (2014) conducted some laboratory tests in a calm air chamber containing DPM and mineral dust concentrations that may be typical of a mine environment. They used a small electrostatic precipitator (ESPnano; DASH Connector Technology, Spokane, WA) to collect samples of the airborne particles. The precipitator creates an electric field that charges the particles and simultaneously deposits them onto

a collection plate. This enables the determination of whether particles can interact in the ambient air; if particles deposit together, they likely occurred together in the air, rather than being forced together during sampling (Miller, Frey, King, & Sunderman, 2010). Based on microscopy analysis, Cauda, Miller, et al., (2014) concluded that some DPM and dust particles were indeed coagulating in the chamber.

Mixed aerosols, in general, and the attachment of DPM and dust, in particular, have not been widely investigated. Beyond the possibility for underestimation of DPM by typical sampling procedures, there may be unique health implications. For example, while some mine dusts (e.g., limestone) are generally regarded as minor respiratory irritants (NIOSH, 2016), the synergistic or antagonistic effects of DPM and dust co-exposures or DPM-laden dust exposures are not known (NASEM, 2018). Indeed, only a few studies exist that specifically examine co-exposures to mine particulates (e.g., CDC, 1984; Karagianes, Palmer, & Busch, 1981).

The purpose of this field study was to explore the possibility of DPM and dust attachment in an operating stone mine. The experimental design combined two types of sampling and analysis: the collection of submicron, respirable, and total particulates for 5040 analysis to determine effective size fractions of DPM, and the collection of ambient particulates for microscopic analysis to identify specific instances of attachment.

## 2. Materials and methods

### 2.1. Study site

This study was conducted in a large-opening underground stone mine, which uses an all-diesel fleet (e.g., haul trucks, loaders, drills, light-duty vehicles). The diesel fleet consists of Tier II and III type engines as well as various diesel particulate filters (DPFs). Due to the challenging ventilation conditions, DPM concentrations in some locations can reach relatively high levels (e.g., 400  $\mu\text{g}/\text{m}^3$  or more as TC) during peak periods. Dust is generally not considered an occupational hazard in the mine. Dust is dominated by carbonate minerals, silica content is negligible, and total respirable dust concentrations are generally less than 1  $\text{mg}/\text{m}^3$  except just adjacent to the primary crusher.

Three sampling locations were selected for the study based on prior observations of DPM and dust (Table 1). The goal was to take samples in locations with significant DPM, but with different dust concentrations. In each location, samples were collected during a single event (i.e., on three different days). Each sampling event was for a period of approximately 5 h, which coincided with a regular production shift to ensure typical DPM and dust conditions. Particulate samples were also collected in each location for subsequent microscopy analysis. Sample collection and analytical procedures are described in detail below.

During DPM sample collection, a TSI 3330 Optical Particle Sizer (OPS) (TSI Inc., Shoreview, MN) was also used to profile dust particle number concentration and size distribution. The OPS reports particle number concentrations in 16 size bins between 0.3 and 10  $\mu\text{m}$ ; but only the 11 bins between 1 and 10  $\mu\text{m}$  were considered here, so that any influence of DPM could be minimized. The average number concentration (#/cc)

of particles between 1 and 10  $\mu\text{m}$  in Locations 1, 2, and 3 were 17.70, 51.83, and 3.23, respectively. Assuming spherical calcite particles ( $\text{SG} = 2.7$  per NIOSH, 2016) with diameters corresponding to the mean size of each bin, the mass concentration of dust in the 1–10  $\mu\text{m}$  size range could be estimated.

## 2.2. 5040 sample collection and analysis

Three sampling trains were used to collect particulate samples for TC and EC assessment (Fig. 1). Similar to other studies (e.g., Noll et al., 2013; Vermeulen et al., 2010), one train was used for total particulates, one was used for respirable particulates, and one was used for “sub-micron” particulates. For sampling total particulates, a closed-face three-piece filter cassette was used with no size selector. For respirable particulates, a two-piece cassette was used with a 10-mm Dorr-Oliver cyclone. For submicron particulates, a DPMI (0.8- $\mu\text{m}$  cut size) and 10-mm Dorr-Oliver cyclone were used; this is a typical setup for DPM sampling in mines. In all cases, Escort ELF pumps (Zefon International Inc., Ocala, FL) were used at a flow rate of 1.7 LPM, and flow rates were checked before and after sample collection.

In each sampling location, triplicate samples were collected with each sampling train. All samples were collected on pre-baked Tissuquartz™ filters (2500 QAT-UP, 37 mm; Pall Corporation, Port Washington, NY) as required by the 5040 standard method. Both primary (i.e., particulates) and secondary (i.e., adsorbed OC) filters were collected so that OC results – and hence TC results – could be corrected to represent particulate OC only (Birch, 2016).

The samples were analyzed using the NIOSH 5040 method. To prepare samples for the analysis, two punches (1.5  $\text{cm}^2$ ) were taken from each primary filter and a single punch was taken from each secondary filter. One of the primary filter punches and the secondary filter punches were analyzed directly using a Sunset Laboratory Inc. Lab OC-EC Aerosol Analyzer (Tigard, OR). The other primary filter punches were acidified prior to 5040 analysis in order to remove carbonate carbon per the method described by Birch (2016). Approximately 25 mL of 37% HCl was added to a glass petri dish and placed in the bottom of a desiccator equipped with a ceramic tray and lid. Once the desiccator environment had sufficient acid vapor (i.e., pH of about 2), the filter punches were placed inside for approximately 1 h.

The 5040 analyzer outputs the following results for each filter punch: OC, EC, and TC as  $\mu\text{g}/\text{cm}^2$ . For the primary punches that were not acidified, the OC and TC results were not corrected for carbonate carbon (i.e., using its thermogram peak); thus, the results reported here include this carbon and therefore appear relatively high. For the acidified punches, the carbonate carbon was removed by the acid prior to 5040 analysis, so the OC and TC have been corrected. As mentioned above, all OC results were corrected to remove the adsorbed OC so that only particulate OC is reported. This was done using the corresponding secondary filter punch.

In order to calculate the concentration of each constituent (OC, EC, or TC) in the sampled environment (i.e., as  $\mu\text{g}/\text{m}^3$ ), the mass per filter area results were converted using the total filter area (i.e., 8.5  $\text{cm}^2$ ), the sampling flow rate, and the sampling time.

### 2.3. TEM sample collection and analysis

In each sampling location, ambient particulates were sampled for later analysis by transmission electron microscopy (TEM). For this, the ESPnano electrostatic precipitator mentioned above was used. This device operates at a very low flow rate of 100 cc/min and the sampling time is programmed by the user depending on the expected particulate concentrations in the sampling environment (Miller et al., 2010). Preliminary tests indicated that sampling for several minutes was sufficient for collecting enough particles for TEM analysis, without overloading the TEM grid. Samples were collected onto 400 mesh copper grids with an ultrathin carbon film on lacey carbon support (Ted Pella Inc., Redding, CA). Fig. 2 shows the ESPNano's sample collection "key" with a TEM grid-mounted.

TEM analysis was conducted on a JEOL 2100 instrument, which is a thermionic emission microscope with a high-resolution pole piece (JEOL Ltd., Akishima, Tokyo, Japan). It is equipped with a large solid angle energy dispersive spectroscopy (EDS) detector, manufactured by JEOL. For each sampling location, the aim was to qualitatively assess the grid samples for particle loading and variety, and then to identify 15–20 particles. Following initial analysis on particles from Location 2, it was clear that the opportunity to observe DPM and dust attachment was most likely in this location (i.e., near the crusher) so additional grids – again collected during regular mine production activities – were explored from there. In total, 10 samples were analyzed and TEM work was limited to about 2 h on each.

To select particles for identification, the strategy was to begin analysis in the upper left quadrant of a grid at about  $50,000\times$  magnification, and gradually move from left to right and top to bottom of the sample. Then, usually three particles were selected for identification and analysis at higher magnification before moving to another frame of view. Since the objective of this work was to assess the possibility of DPM and dust attachment, particles suspected to be dust were prioritized for analysis over those that were suspected to be DPM (based on characteristic morphology and graphitic layers (i.e., as reported by Ishiguro, Takatori, & Akihama, 1997)). Elemental mapping or spectral analysis was also conducted by EDS to enable the identification of dust particles. TEM results were catalogued by sampling location, particle type and size.

## 3. Results and discussion

Using the OPS data, dust concentrations in the 1–10  $\mu\text{m}$  range were estimated in each sampling location (Table 2). As expected, the highest dust concentration was in Location 2, which was adjacent to the primary crusher and main mine exhaust. Location 1 had moderate dust concentration near the active production area (i.e., where mined material was being actively loaded into haul trucks). Location 3 was only affected by intermittent light duty traffic and stationary diesel pumps, and thus had very low dust concentration. It should be reiterated that the OPS-derived values are only estimates, based on very cursory assumptions used to transform number concentrations into mass concentrations. However, the observed trend is supported by the 5040 results from the total particulate samples. To explain, since dust in the mine should be dominated by carbonate minerals, the difference between

acidified and non-acidified TC concentrations in a particular location should provide another measure of dust concentration (see Figs. 3 and 4).

With respect to DPM, the highest 5040 EC concentrations were observed in Location 1, followed by Location 2 and then Location 3 (results from the acidified samples shown in Fig. 3). This is consistent with expectations, considering the mine activities in the vicinity of each sampling location. Significant differences could generally not be observed between 5040 EC in the three size ranges sampled. There was substantial variability between the triplicate results. As this occurred across all size ranges and for both acidified and non-acidified samples (Figs. 3 and 4), it is most likely related to spatial variability in the sampled environments rather than factors associated with sampling equipment (e.g., cassette types, specific pumps) or mine dust interference. Spatial variability is indeed a well-known issue for the collection of airborne particulate samples in mine environments (e.g., see Kissell & Sacks, 2002, and Vinson, Volkwein, & McWilliams, 2007).

The fact that total, respirable, and submicron EC concentrations were observed to be similar within each sampling location indicates that, on a mass basis, the mine studied simply does not have considerable DPM that occurs in the supramicron range. This finding is contrary to data from many mines (e.g., Vermeulen et al., 2010), which have shown that supramicron particles can contribute significantly to the total DPM mass (i.e., using EC as a surrogate), but is not unprecedented. For instance, Maximilien et al. (2017) reported that most DPM in two underground gold mines resided in the submicron range. Variability in the ratio between submicron and respirable EC (or TC) in different mines is likely related to specific equipment or operating conditions. Exhaust after-treatment technologies such as DPFs, for instance, are known to effectively change the particle size distribution of DPM (Lee, Goto, & Odaka, 2002).

While there was apparently not a significant amount of supramicron DPM in the study mine, the results presented here could support respirable (instead of submicron) DPM sampling in mine environments where the primary mineral dust interference of concern is from carbonates. Such an approach would require carbonate removal by sample acidification (i.e., as done here) or analytically by integration of the carbonate peak on the 5040 thermogram. However, this would allow for the accounting of any oversized DPM that is excluded by typical submicron sampling.

Furthermore, the results presented here add to a number of others that suggest the use of EC (rather than TC) as a DPM surrogate in mines, based on the ability to more easily measure EC and the possibility of TC interferences from non-DPM sourced OC or carbonate carbon (e.g., see Noll et al., 2007; Noll, Mischler, Schnakenberg Jr. & Bugarski, 2006). For diesel exhaust exposure assessments in non-metal mines, Vermeulen et al. (2010) also concluded that respirable EC is an appropriate analytical surrogate. They noted that, due to a strong observed correlation between respirable and submicron EC in their study mines (i.e., a median submicron EC to respirable EC ratio of 0.77 with a Pearson coefficient of 0.94), either quantity could be a suitable surrogate. However, the fact that submicron and respirable EC have a much different ratio in the current study (i.e., they are about equal, but still well correlated) highlights the favorability of respirable EC – or the need to determine

a mine-specific submicron to respirable ratio if the submicron surrogate is to be used. This way, supramicron DPM is not missed by sampling efforts, or can at least be accounted for using a mine-specific correction factor.

Although the 5040 results indicated that DPM and respirable dust attachment in the study mine atmosphere must not substantially influence typical DPM mass measurements, the TEM results showed that such attachment does indeed occur. Table 3 summarizes the particles identified on each of the TEM sample grids analyzed for this study.

In Location 1 near the production activities, the majority of particles observed on the grid were DPM agglomerates (Fig. 5). These ranged in size from about 0.05  $\mu\text{m}$  to 0.5  $\mu\text{m}$  in the longest dimension viewable, and occurred in a variety of shapes from long chains to large clusters. Dust particles were also observed on the TEM grid (Fig. 6). Five of these particles were selected for analysis using EDS, which revealed that two were carbonate, two were Ti-rich, and one appeared to be silica. No dust particles were found to have attached to DPM in Location 1.

In the more remote Location 3, no dust particles could be found on the TEM sample. However, many DPM agglomerates were observed (Fig. 7). While the DPM again ranged in size, qualitatively it appeared to be larger in this location than in Location 1. This may be related to the specific source(s) of DPM. Location 3 is expected to be influenced to some extent by emissions from the production area, though a diesel water pump running near the sampling location was the likely source of most of the DPM. Evidence of high humidity in this area was also seen during the TEM work. In some cases, small spots indicative of evaporated water drops were observed around the DPM clusters (Fig. 8). In two instances, Cu-rich particles were observed with DPM surrounding them (Fig. 6). Given that significant copper content is not expected in dust generated in the mine, these particles are suspected to be copper salts precipitated following the deposition of DPM agglomerates with condensed water on the copper TEM grid.

In Location 2 near the primary crusher and main exhaust, both DPM and dust particles were found on the TEM samples. On the samples with the lightest particle loading, only DPM particles could generally be observed, and no particles were found on one sample, which may mean that something went wrong during sample collection. As in Location 3, DPM particles appeared to be relatively large. Two samples were considered to be densely loaded, and most of the dust particles were found in these. Notably, all dust particles selected for analysis were observed to have attached DPM. The DPM appeared to completely surround the dust particle in some cases (Figs. 9 and 10), and was attached just to the particle edge in others (Fig. 11). EDS spectra indicated that the dust particles were of several different mineral types, including carbonates and alumino-silicates. Some of the particles were in the submicron range, but others were larger. Due to the lower limits on magnification in the TEM, larger particles could not be measured.



## 4. Conclusions

By pairing mass measurements of EC in different size fractions with microscopy analysis, this study sought to investigate the possibility of DPM and dust attachment in an underground stone mine. Such attachment may have implications for both DPM sampling and exposure outcomes. Based on the 5040 sample results, a significant fraction of EC was not observed to occur in the supramicron range, but the TEM results did confirm that DPM and dust can attach to some extent in the mine atmosphere. It is important to note that the TEM work undertaken here was exploratory in that the aim was to see if attachment could be observed, rather than an attempt to quantify its frequency. The strategy employed for the current study could be adapted for future investigations.

## Acknowledgements

This work was supported by the CDC/NIOSH (Contract Number: 200-2014-59646). Sincere thanks also to Shawn Vanderslice of NIOSH for sample analysis, Chris Winkler of Virginia Tech ICTAS-NCFL for assistance with the TEM work, Chelsea Barrett for helping with equipment setup, and all the personnel at the study mine for their interest and support.

## References

- Abdul-Khalek IS, Kittelson DB, Graskow BR, Wei Q, & Bear F (1998). Diesel exhaust particle size: Measurement issues and trends. SAE technical paper. 10.4271/980525.
- Birch ME (2016). Monitoring of diesel particulate exhaust in the workplace. NIOSH Manual of Analytical Methods (NMAM) (5th ed.). Retrieved September 1, 2018 from <https://www.cdc.gov/niosh/docs/2014-151/pdfs/chapters/chapter-dl.pdf>.
- Bukowiecki N, Kittelson DB, Watts WF, Burtscher H, Weingartner E, & Baltensperger U (2002). Real-time characterization of ultrafine and accumulation mode particles in ambient combustion aerosols. *Journal of Aerosol Science*, 33(8), 1139–1154. 10.1016/S0021-8502(02)00063-0.
- Cantrell BK, & Rubow KL (1991). Development of personal diesel aerosol sampler design and performance criteria. *Mining Engineering*, 43(2), 232–236.
- Cantrell BK, & Watts WF (1997). Diesel exhaust aerosol: Review of occupational exposure. *Applied Occupational and Environmental Hygiene*, 12(12), 1019–1027. 10.1080/1047322X.1997.10390643.
- Cauda E, Miller A, Stabile L, & Buonanno G (2014). Characterizing the exposure of miners to mixed aerosols. Proceedings of the international conference on atmospheric dust. Taranto, Italy, June 1–6, 2014, (pp. x–x). City: Publisher.
- Cauda E, Sheehan M, Gussman R, Kenny L, & Volkwein J (2014). An evaluation of sharp cut cyclones for sampling diesel particulate matter aerosol in the presence of respirable dust. *Annals of Occupational Hygiene*, 58(8), 995–1005. 10.1093/annhyg/meu045. [PubMed: 25060240]
- CDC (1984). Centers for Disease Control. Chronic inhalation exposure to coal dust and/or diesel exhaust: Effects on the alveolar macrophages of rats. *Morbidity and Mortality Weekly Report*, 33(7), 101–102. [PubMed: 6422247]
- Chou CC-K, Chen T-K, Huang S-H, & Liu SC (2003). Radiative absorption capability of asian dust with black carbon contamination. *Geophysical Research Letters*, 30(12), 1616. 10.1029/2003GL017076.
- Gaillard S, Sarver E, & Cauda E (2018). Impact of aging on performance of impactor and sharp-cut cyclone size selectors for DPM sampling. *Mining Engineering*, 70(8), 43–49. 10.19150/me.8428. [PubMed: 30686842]
- Ishiguro T, Takatori Y, & Akihama K (1997). Microstructure of diesel soot particles probed by electron microscopy: First observation of inner core and outer shell. *Combustion and Flame*, 108(1–2), 231–234. 10.1016/S0010-2180(96)00206-4.

- Karagianes M, Palmer R, & Busch R (1981). Effects of inhaled diesel emissions and coal-dust in rats. *American Industrial Hygiene Association Journal*, 42(5), 382–391. [PubMed: 6164283]
- Kissell F, & Sacks H (2002). Inaccuracy of area sampling for measuring the dust exposure of mining machine operators in coal mines. *Mining Engineering*, 54(2), 33–39.
- Kittelson D (1998). Engines and nanoparticles: A review. *Journal of Aerosol Science*, 29(5–6), 575–588. 10.1016/S0021-8502(97)10037-4.
- Lee J, Goto Y, & Odaka M (2002). Measurement of the diesel exhaust particle reduction effect and particle size distribution in a transient cycle mode with an installed diesel particulate filter (DPF). *SAE Transactions*, 111, 370–376. 10.4271/2002-01-1005.
- Maximilien D, Couture C, Njanga P-E, Neesham-Grenon E, Lachapelle G, Coulombe H, et al. (2017). Diesel engine exhaust exposures in two underground mines. *International Journal of Mining Science and Technology*, 267(4), 641–645. 10.1016/j.ijmst.2017.05.011.
- Miller A, Frey G, King G, & Sunderman C (2010). A handheld electrostatic precipitator for sampling airborne particles and nanoparticles. *Aerosol Science and Technology*, 44(6), 417–427. 10.1080/02786821003692063.
- MSHA (2008). Mine Safety and Health Administration. Diesel particulate matter exposure of underground metal and nonmetal miners. Rules and Regulations, Federal Register 30 CFR Part 57, 73(98), 29058–29060. Retrieved September 1, 2018 from <https://www.govinfo.gov/content/pkg/FR-2008-05-20/pdf/E8-11329.pdf>.
- NASEM (2018). National academies of sciences, engineering and medicine. Monitoring and sampling approaches to assess underground coal mine dust exposures Washington, DC: The National Academies Press 10.17226/25111.
- NIOSH (2016). National Institute of occupational safety and health. Limestone. NIOSH pocket Guide to chemical hazards. Retrieved September 1, 2018 from <https://www.cdc.gov/niosh/npg/npgd0369.html>.
- Noll JD, Bugarski AD, Patts LD, Mischler SE, & McWilliams L (2007). Relationship between elemental carbon, total carbon, and diesel particulate matter in several underground metal/non-metal mines. *Environmental Science and Technology*, 41(3), 710–716. 10.1021/es061556a. [PubMed: 17333567]
- Noll JD, Janisko S, & Mischler SE (2013). Real-time diesel particulate monitor for underground mines. *Analytical Methods*, 5(12), 2954–2963. 10.1039/C3AY40083B.
- Noll JD, Mischler SE, Schnakenberg GH Jr., & Bugarski AD (2006). Measuring diesel particulate matter in underground mines using sub micron elemental carbon as a surrogate. *Proceedings of the 11th US/north American mine ventilation symposium*, 5–7 June 2006, Pennsylvania, USA (pp. 105–110). London: Taylor & Francis.
- Noll JD, Timko RJ, McWilliams L, Hall P, & Haney R (2005). Sampling results of the improved SKC diesel particulate matter cassette. *Journal of Occupational and Environmental Hygiene*, 2(1), 29–37. 10.1080/15459620590900320. [PubMed: 15764521]
- Pietikainen M, Oravisjarvi K, Rautio A, Voutilainen A, Ruuskanen J, & Keiski RL (2009). Exposure assessment of particulates of diesel and natural gas fueled buses in silico. *The Science of the Total Environment*, 408, 163–168. [PubMed: 19828175]
- Vermeulen R, Coble JB, Yereb D, Lubin JH, Blair A, Portengen L, et al. (2010). The diesel exhaust in miners study: III. Interrelations between respirable elemental carbon and gaseous and particulate components of diesel exhaust derived from area sampling in underground non-metal mining facilities. *Annals of Occupational Hygiene*, 54(7), 762–773. 10.1093/annhyg/meq023. [PubMed: 20876234]
- Vinson R, Volkwein J, & McWilliams L (2007). Determining the spatial variability of personal sampler inlet locations. *Journal of Occupational and Environmental Hygiene*, 4(9), 708–714. 10.1080/15459620701540618. [PubMed: 17654226]

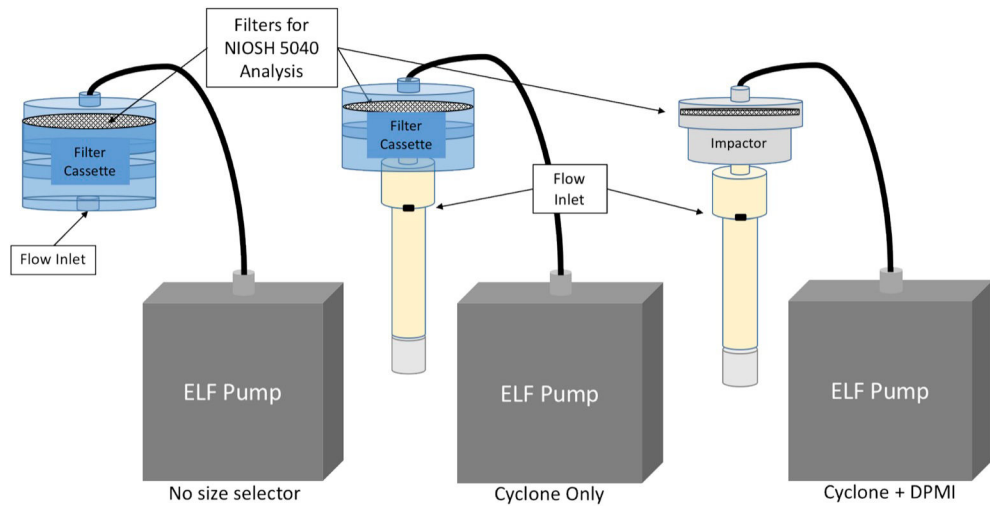


**Fig. 1.** Three sampling trains to collect particulates in different size ranges. The “no size selector” train was used to collect total airborne particulates. The “cyclone only” train was used to collect respirable particulates. The “cyclone + DPPI” train was used to collect submicron ( $< 0.8 \mu\text{m}$ ) particulates.



**Fig. 2.**  
ESPnano key with an affixed copper mesh TEM grid.

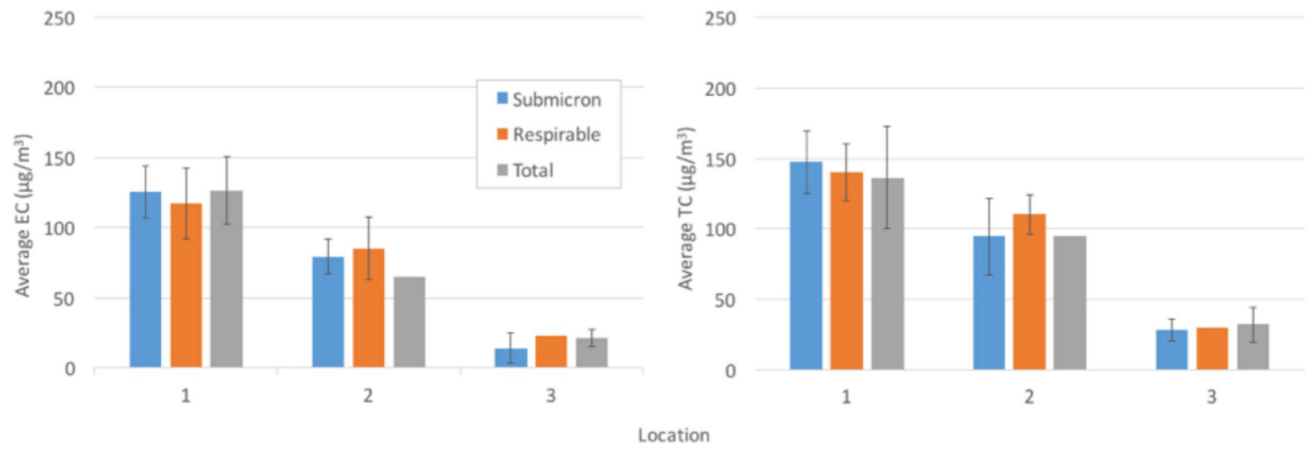


**Fig. 3.**

Average EC (left) and TC (right) concentrations in each monitoring location as determined from the acidified samples. Error bars represent 95% confidence intervals. (Note that confidence intervals could not be determined for total particulate results in Location 2 and respirable results in Location 3 due to a missing triplicate sample result in both of these sets).

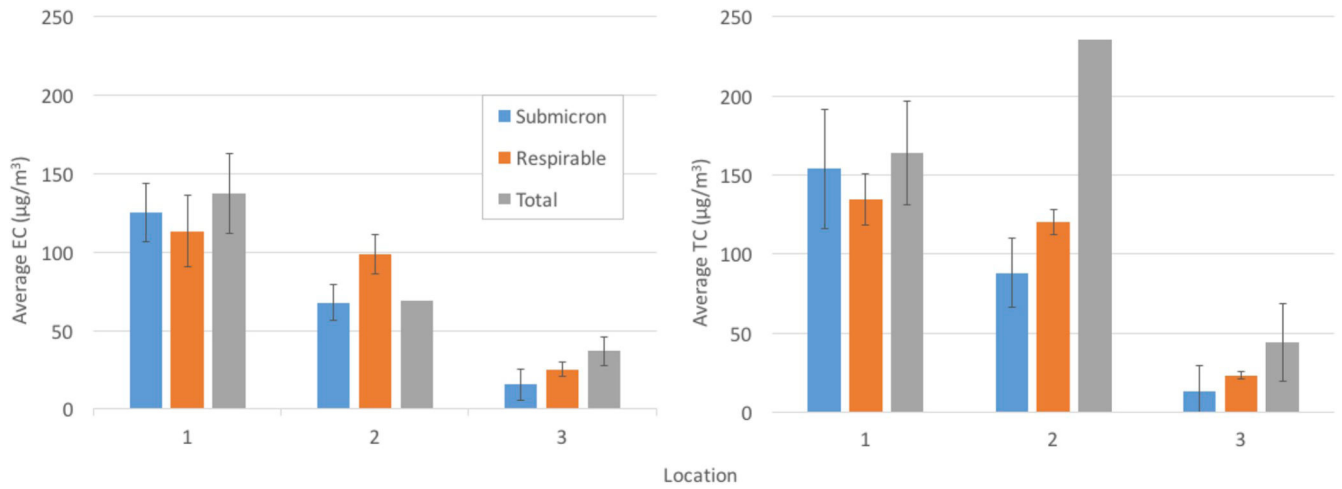


**Fig. 4.** Average EC (left) and TC (right) concentrations in each monitoring location as determined from the non-acidified samples; where present, carbonate dust can cause TC to be overestimated by the standard 5040 analysis. Error bars represent 95% confidence intervals. (Note that confidence intervals could not be determined for total particulates in Location 2 due to a missing triplicate sample result).

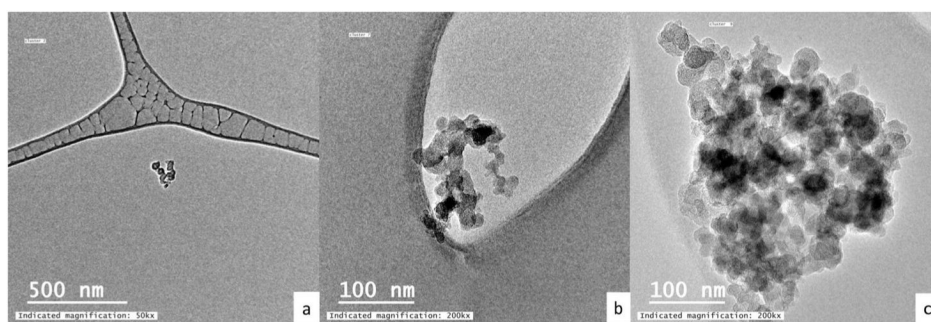


**Fig. 5.** TEM images of DPM agglomerates collected in Location 1 (a)  $\sim 0.125 \mu\text{m}$ , (b)  $\sim 0.15 \mu\text{m}$ , (c)  $\sim 0.05 \mu\text{m}$ ).

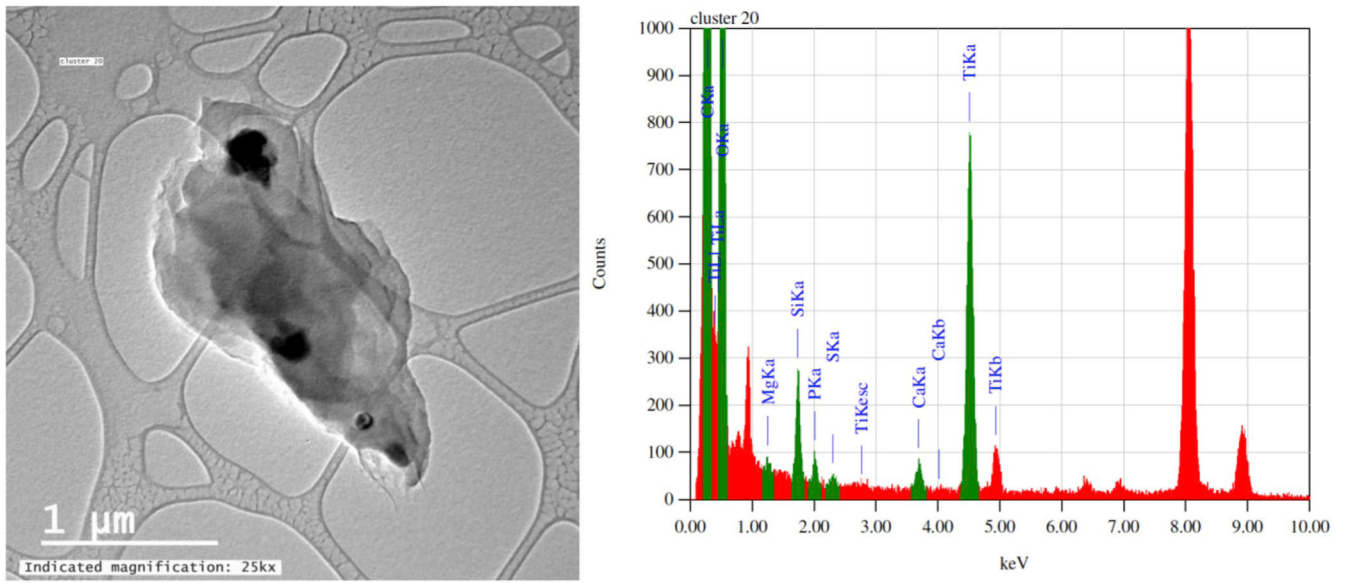


**Fig. 6.** TEM image and EDS spectra of a Ti-rich dust particle collected in Location 1 (~2.0 μm).



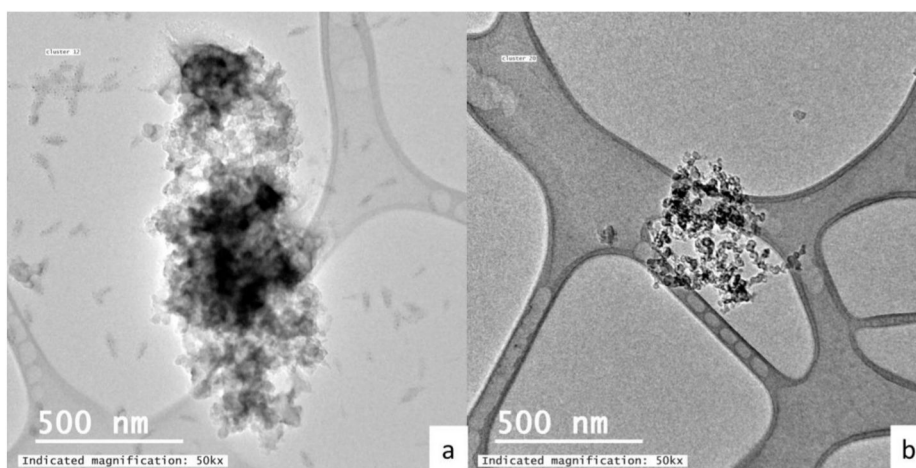


**Fig. 7.** TEM images of DPM agglomerates collected in Location 3 (a)  $\sim 1.25 \mu\text{m}$ , (b)  $\sim 0.5 \mu\text{m}$ ).

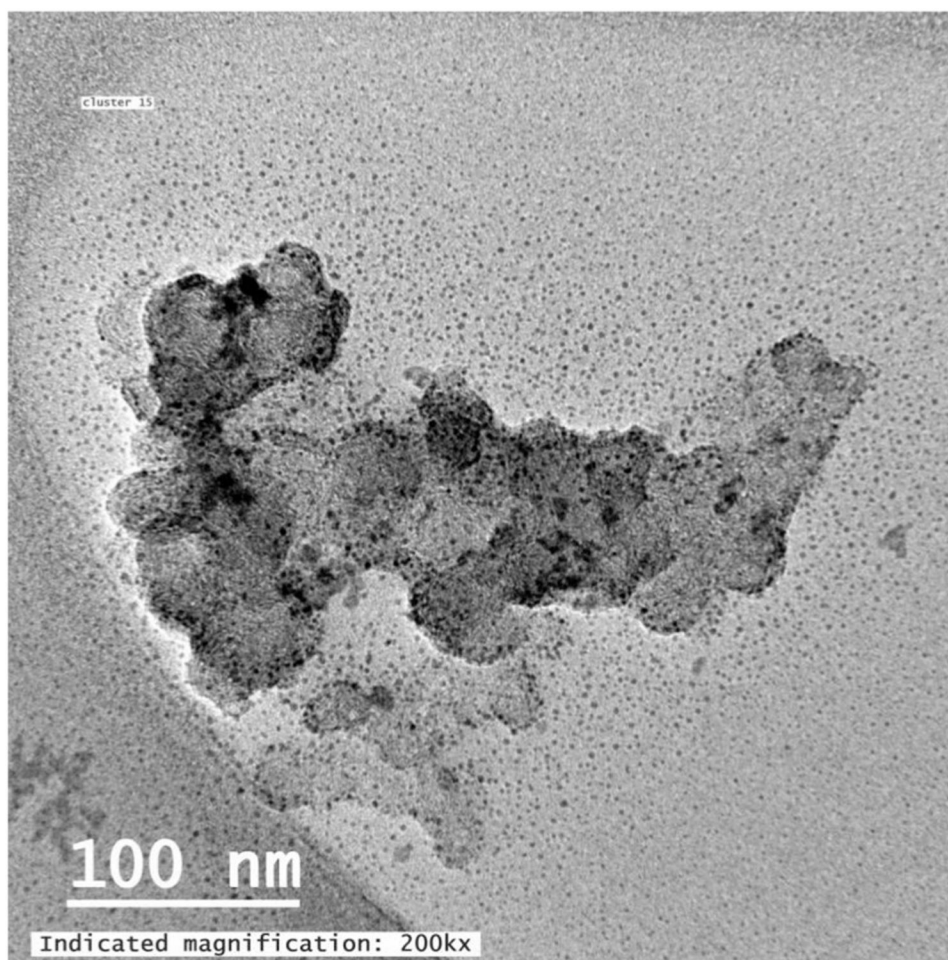


**Fig. 8.** TEM image of DPM from Location 3 ( $\sim 0.3 \mu\text{m}$ ). The small dark spots are interpreted as evaporated water droplets containing precipitated Cu.

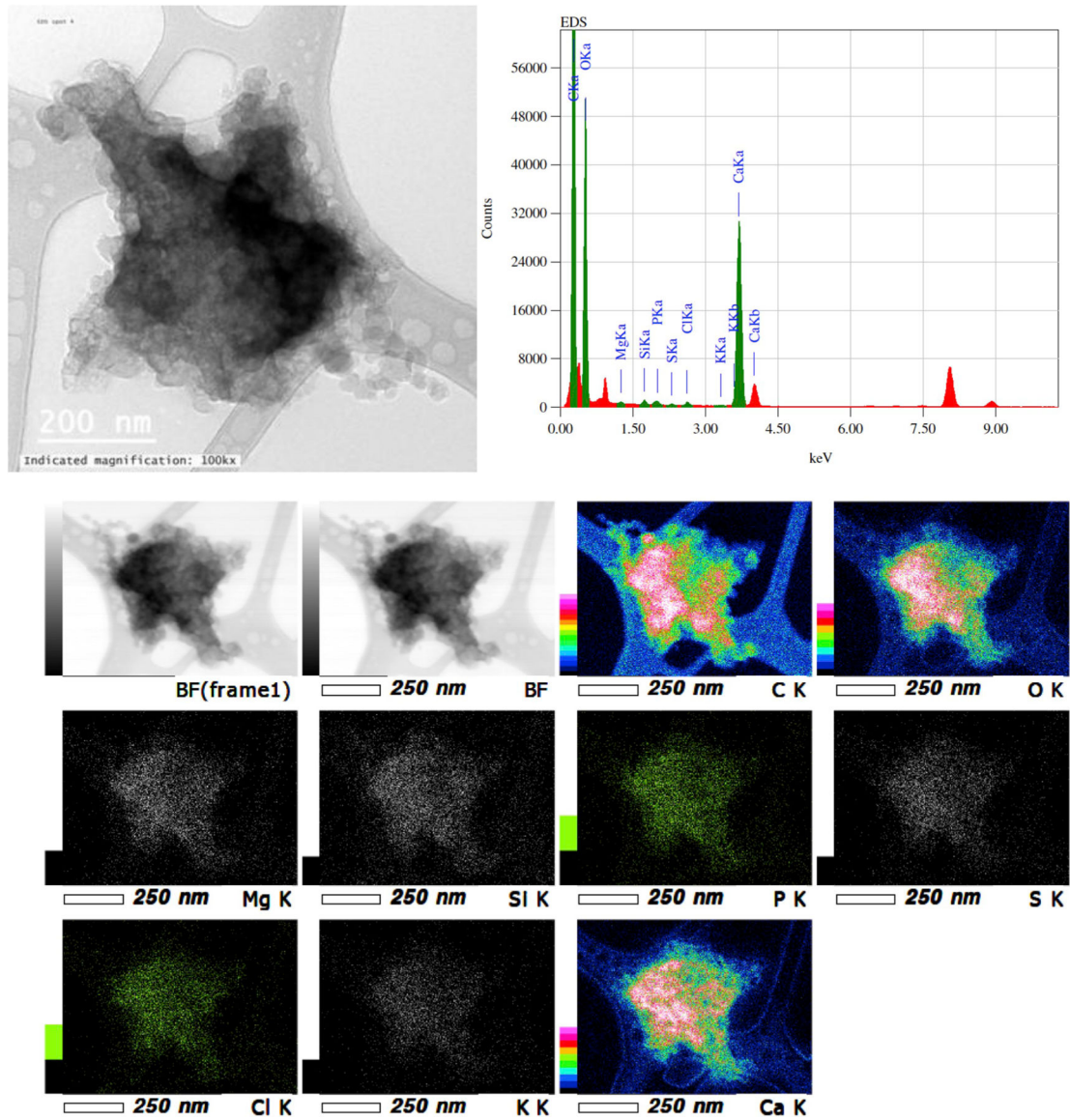


**Fig. 9.**  
 TEM image, EDS spectra, and element map of DPM surrounding a carbonate dust particle from Location 2 (~0.7 μm).

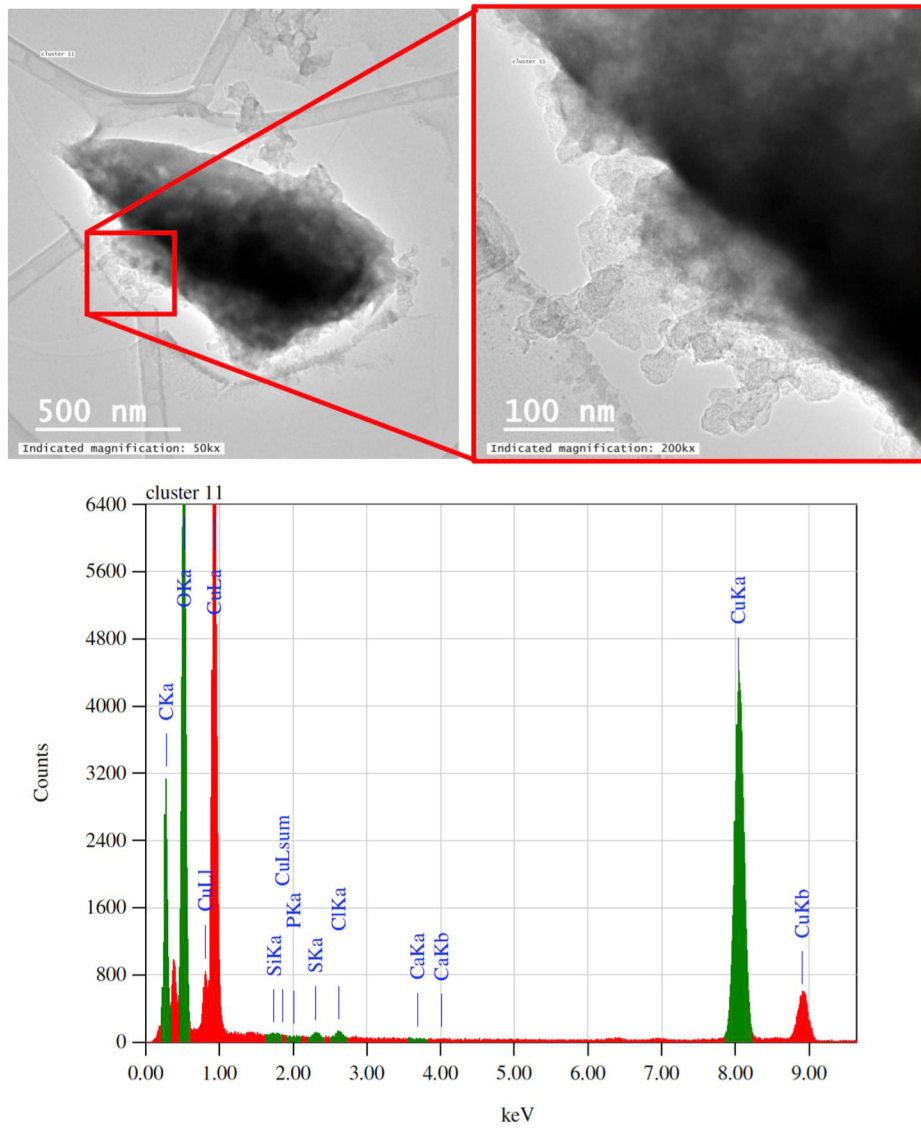


**Fig. 10.** TEM image and EDS spectra of a Cu-rich particle with DPM surrounding it from Location 3 (~0.2  $\mu\text{m}$ ).

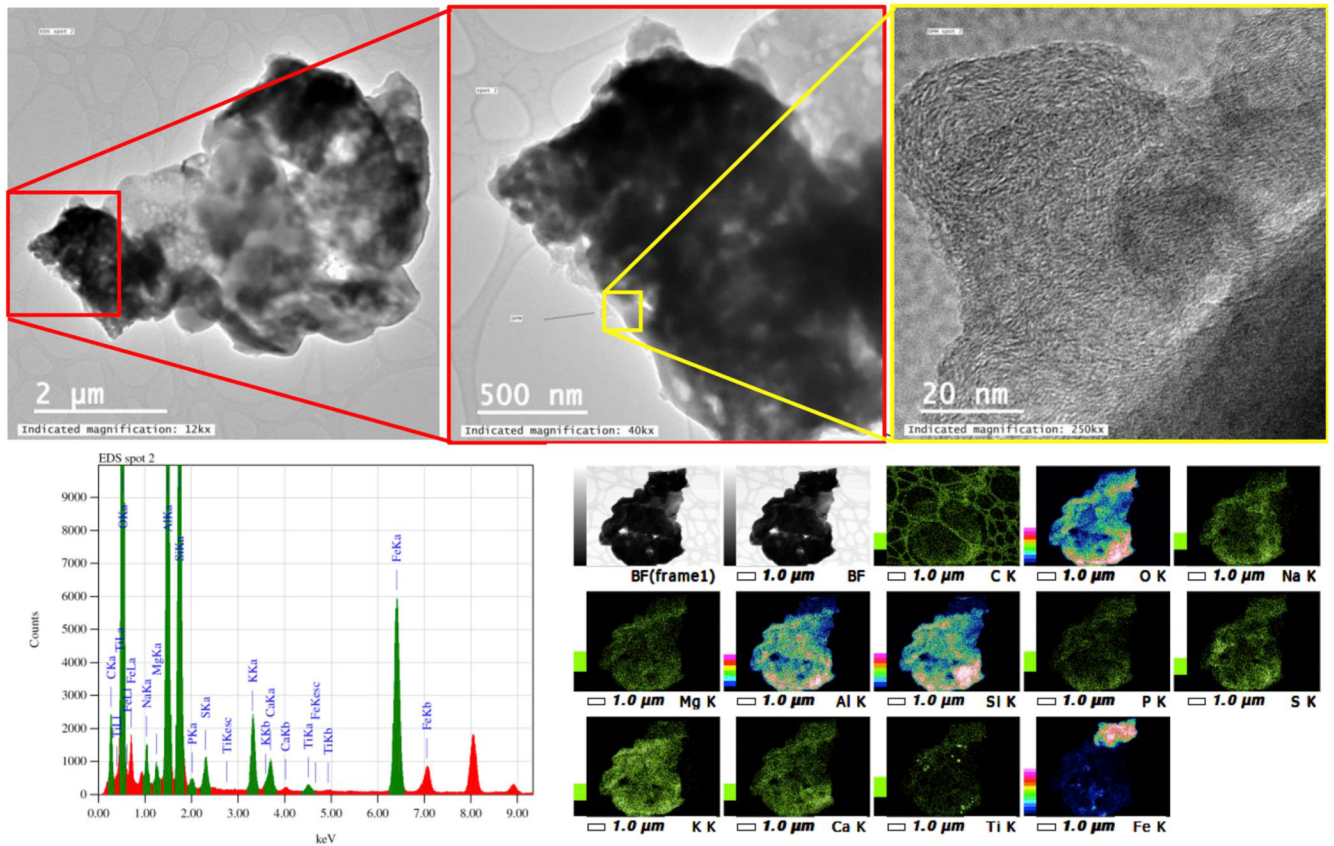


**Fig. 11.** TEM image, EDS spectra, and element map of DPM on the edges of a large alumino-silicate dust particle from Location 2 (~6.0 μm).

**Table 1**

Description and summary of monitoring locations in the study mine.

| Location | Description   |
|----------|---|
| 1        | Near primary production zone (moderate dust, high DPM)  |
| 2        | Near main mine exhaust and primary crusher (high dust, high DPM)                                      |
| 3        | Remote location with respect to production, but near stationary diesel pumps (low dust, moderate DPM) |

Author Manuscript

Author Manuscript

Author Manuscript

Author Manuscript

**Table 2**

Estimated dust mass concentration in the 1–10  $\mu\text{m}$  range based on OPS number concentration data.

| Location of sampling | Estimated dust mass ( $\text{mg}/\text{m}^3$ ) |
|----------------------|--|
| 1                    | 0.78   |
| 2                    | 3.86   |
| 3                    | 0.08   |

Author Manuscript

Author Manuscript

Author Manuscript

Author Manuscript

**Table 3**

Summary of particles analyzed by TEM in each sampling location.

| Location | Sample No. | Sample time (seconds) | Particle loading | Total particles analyzed | DPM | DPM on dust | Dust |
|----------|------------|-----------------------|------------------|--------------------------|-----|-------------|------|
| 1        | 1.1        | 200                   | High             | 19                       | 14  | 0           | 5    |
| 2        | 2.1        | 200                   | High             | 25                       | 16  | 9           | 0    |
|          | 2.2        | 2                     | Low              | 1                        | 1   | 0           | 0    |
|          | 2.3        | 10                    | Low              | 3                        | 2   | 1           | 0    |
|          | 2.4        | 100                   | High             | 10                       | 3   | 7           | 0    |
|          | 2.5        | 200                   | Low              | 0                        | 0   | 0           | 0    |
|          | 2.6        | 200                   | Low              | 1                        | 1   | 0           | 0    |
|          | 2.7        | 200                   | Low              | 2                        | 2   | 0           | 0    |
|          | 2.8        | 200                   | Low              | 1                        | 0   | 1           | 0    |
| 3        | 3.1        | 200                   | High             | 17                       | 17  | 0           | 0    |